ISSN 1023-1935, Russian Journal of Electrochemistry, 2018, Vol. 54, No. 6, pp. 459–463. © Pleiades Publishing, Ltd., 2018.
Original Russian Text © D.A. Agarkov, M.A. Borik, S.I. Bredikhin, A.V. Kulebyakin, I.E. Kuritsyna, E.E. Lomonova, F.O. Milovich, V.A. Myzina, V.V. Osiko, E.A. Agarkova, N.Yu. Tabachkova, 2018, published in Elektrokhimiya, 2018, Vol. 54, No. 6, pp. 530–535.

Structure and Transport Properties of Zirconia-Based Solid Solution Crystals Co-Doped with Scandium and Cerium Oxides[1]

D. A. Agarkov[a], M. A. Borik[b], S. I. Bredikhin[a], A. V. Kulebyakin[b], I. E. Kuritsyna[a], E. E. Lomonova[b], F. O. Milovich[c], V. A. Myzina[b], V. V. Osiko[b], E. A. Agarkova[a], and N. Yu. Tabachkova[c, *]

[a] *Institute of Solid State Physics, Russian Academy of Sciences, Chernogolovka, Moscow oblast, 142432 Russia*
[b] *Prokhorov Institute of General Physics, Russian Academy of Sciences, Moscow, 119991 Russia*
[c] *National University of Science and Technology MISiS, Moscow, 119049 Russia*
**e-mail: ntabachkova@gmail.com*

Received September 4, 2017; in final form, January 12, 2018

Abstract—The crystals of $(ZrO_2)_{1-x}(Sc_2O_3)_x(CeO_2)_{0.01}$ solid solutions (x = 0.08–0.10) were obtained by directional crystallization. The crystals of the grown composites were semitransparent, opalescent, and without cracks and had varying microstructure in the bulk. In the range of compositions under study, it was impossible to obtain optically homogeneous, fully transparent crystals. The crystals grown at a growth rate of 10 mm/h had a nonuniform distribution of ceria along the length of the ingot. The introduction of ceria in an amount of 1 mol % increased the conductivity of the crystals, but the increase in the specific electric conductivity depended on the Sc_2O_3 content and the phase composition of the crystals. The highest conductivity was inherent in the $(ZrO_2)_{0.89}(Sc_2O_3)_{0.10}(CeO_2)_{0.01}$ crystals.

Keywords: solid electrolytes, zirconia, single crystals, phase composition, structure, ion conductivity, mechanical properties

DOI: 10.1134/S1023193518060022

INTRODUCTION

The materials based on zirconia are widely used as solid electrolytes for solid oxide fuel cells (SOFCs) [1, 2]. One of the important applied problems is the development of new materials with the highest ion conductivity in order to lower the working temperature of solid electrolytes, which increases their service life, makes the design easier, and lowers the cost of the materials used in the production of SOFCs. From this viewpoint, the Sc_2O_3–CeO_2–ZrO_2 system is one of the most attractive systems with high ion conductivity at temperatures of 900–700°C. Thus, the ceramic material $10Sc_2O_3$–$90ZrO_2$ co-doped with 1 mol % CeO_2 has ion conductivity of 16.7 mS/cm at 600°C [3]. The physicochemical and transport properties of the materials of this system were studied by many authors [4–9]. The ion conductivity of ceramic samples of the same chemical composition (10Sc1CeSZ) depends largely on the phase composition, microstructure, density, and other parameters, which, in turn, are determined by the method for the preparation of the material [10–12]. In particular, the conductivity along the grain boundaries has a great effect on the total ion conductivity of ceramic materials.

The goal of this work was to synthesize the crystals of the Sc_2O_3–CeO_2–ZrO_2 system and study their physicochemical and transport properties. As shown earlier, the total conductivity of these crystalline materials is determined only by their bulk conductivity even in the presence of a twin structure [13]. Therefore, studies of these crystals will allow us to evaluate the contribution of the bulk component of conductivity in the solid electrolyte, excluding the contribution of grain-boundary conductivity, which can significantly simplify the analysis of the mechanisms of ion conductivity.

EXPERIMENTAL

The crystals of $(ZrO_2)_{1-x}(Sc_2O_3)_x(CeO_2)_{0.01}$ solid solutions (x = 0.08–0.10) were obtained by directional crystallization of a melt in a cold container [14]. The $(ZrO_2)_{1-x}(Sc_2O_3)_x$ crystals (x = 0.08–0.10) were also obtained for the sake of comparison.

The chemical composition of the grown crystals was determined on a JEOL 5910 LV scanning electron

[1] Presented at the IV All-Russian Conference "Fuel Cells and Fuel Cell based Power Plants" (with international participation) June 25–29, 2017, Suzdal, Vladimir region.

Table 1. Composition, density, and microhardness of grown crystals

Symbol	Composition	Density, g/cm^3	Microhardness, *HV*, kg/mm^2
8Sc1CeSZ	$(ZrO_2)_{0.91}(Sc_2O_3)_{0.08}(CeO_2)_{0.01}$	5.850 ± 0.003	1660 ± 20
9Sc1CeSZ	$(ZrO_2)_{0.90}(Sc_2O_3)_{0.09}(CeO_2)_{0.01}$	5.791 ± 0.004	1680 ± 20
10Sc1CeSZ	$(ZrO_2)_{0.89}(Sc_2O_3)_{0.10}(CeO_2)_{0.01}$	5.757 ± 0.004	1720 ± 20
8ScSZ	$(ZrO_2)_{0.92}(Sc_2O_3)_{0.08}$	5.862 ± 0.004	1610 ± 20
9ScSZ	$(ZrO_2)_{0.91}(Sc_2O_3)_{0.09}$	5.807 ± 0.001	1640 ± 20
10ScSZ	$(ZrO_2)_{0.89}(Sc_2O_3)_{0.10}$	5.763 ± 0.002	1580 ± 20

microscope with an INCA Energy energy dispersive analyzer (Japan). In measurements of the crystal composition, fused zirconium, scandium, and cerium oxides were used as standards. The XRD analysis was performed on a Bruker D8 diffractometer (Germany) using CuK_α radiation. The Raman spectroscopic study was performed on a Renishaw inVia Raman microscope spectrograph (Great Britain). A laser with a wavelength of 532 nm was used as a source of excitation.

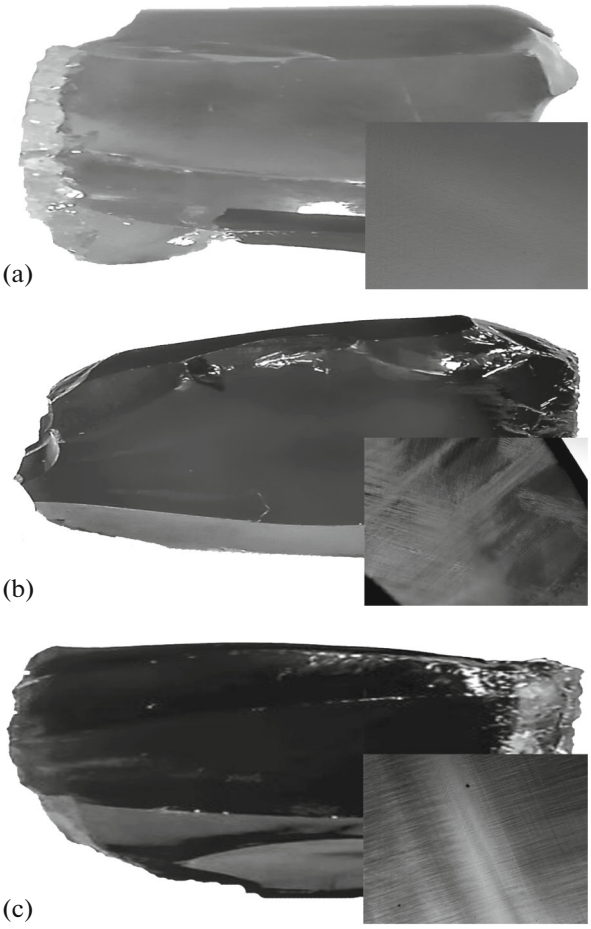

Fig. 1. View of $(ZrO_2)_{1-x}(Sc_2O_3)_x(CeO_2)_{0.01}$ crystals: (a) 8Sc1CeSZ, (b) 9Sc1CeSZ, and (c) 10Sc1CeSZ. Inserts: optical images of microstructure obtained in transmitted light.

The density was determined by hydrostatic weighing on a Sartorius hydrostatic balance (Switzerland). The crystal microhardness was measured on a DM 8 B AUTO microhardness meter (Affri, Italy) at a load of 50 g.

The conductivity of zirconia-based crystals was measured in the temperature range 400–900°C using a Solartron SI 1260 frequency analyzer (Solartron Analytical, United Kingdom) in the frequency range 1 Hz–5 MHz with an AC signal amplitude of 24 mV. Plates with an area of 7 × 7 mm^2 and a thickness of 0.5 mm were used for measurements. To form current contacts, platinum paste was applied to the opposite sides of the crystals and burnt in at 950°C for 1 h in air. The impedance spectra were processed using the ZView program (version 2.8). The specific conductivity of the crystals was calculated from the data obtained by processing the impedance spectra, taking into account the dimensions of the samples.

RESULTS AND DISCUSSION

Table 1 gives the compositions of the grown crystals and the notation used below. The grown crystals were translucent, opalescent, and without cracks and had a shape and dimensions similar to those of zirconia crystals stabilized with scandium and/or yttrium oxides [14, 15]. Figure 1 shows the appearance of the crystals. The inserts show the optical images of microstructure obtained in transmitted light on polished plates 1 mm thick (magnification ×25). The coloring of the crystals co-doped with cerium oxide was nonuniform and varied from colorless to dark orange. The color variation is associated with both the change in the valence state of the cerium ion during the cooling of the crystal after growth and variations in the concentration of the cerium oxide impurity during crystallization. In the first case, the variation manifests itself as a decrease in the color intensity with colorless areas appearing on the surface, which is most typical for crystals growing closer to the periphery of the crystallized melt ingot. This change in color suggests a decrease in the concentration of the trivalent cerium cation, which has absorption bands in the visible region and gives the crystals an orange color [16]. During the cooling of the ingot, a $Ce^{3+} \rightarrow Ce^{4+}$ transi-

Table 2. Phase composition and lattice parameters of the crystals according to the XRD data before and after annealing in air at 1200°C

Sample	Phase composition	Lattice parameters					
		before annealing			after annealing		
		a, nm	c, nm	$c/\sqrt{2}a$	a, nm	c, nm	$c/\sqrt{2}a$
8Sc1CeSZ	t	0.3599	0.5114	1.005	0.3597	0.5123	1.007
9Sc1CeSZ	t	0.3597	0.5110	1.005	0.3597	0.5111	1.005
10Sc1CeSZ	c	0.5093			0.5093		
8ScSZ	t	0.3596	0.5123	1.007	0.3596	0.5123	1.007
9ScSZ	t	0.3595	0.5122	1.007	0.3595	0.5122	1.007
10ScSZ	c	0.5091			0.5091		
	r	0.3562	0.9010		0.3562	0.9010	

c—Cubic modification of ZrO_2; t—tetragonal modification of ZrO_2; r—rhombohedral modification of ZrO_2.

tion occurs as oxygen diffuses from the periphery of the ingot. Annealing of the crystals in air at 400–1200°C makes it possible to eliminate the color nonuniformity and leads to the formation of colorless crystals. Annealing in vacuum at temperatures of the order of 1200–1400°C leads to a $Ce^{4+} \rightarrow Ce^{3+}$ transition and, accordingly, to a homogeneous coloring of the crystals in different shades from orange to dark red depending on the composition [16]. If the varying color is related to variations in the ceria concentration during crystallization, then regions or bands with different intensities arise in crystal due to the displacement of the cerium impurity along the height of the ingot during crystallization, the effective distribution coefficient of the impurity being less than unity [16]. In these cases, the local increase in the ceria concentration is caused by abnormal crystallization because of the concentration overcooling at the crystallization front, which leads to rapid crystallization of the region enriched with the displaced impurity. Thus, it was impossible to obtain optically uniform, transparent crystals of $(ZrO_2)_{1-x}(Sc_2O_3)_x(CeO_2)_{0.01}$ in the range of the compositions under study, in contrast to the case of crystals co-doped with scandium and yttrium oxides [17].

The distribution of scandium and cerium oxides along the length of the crystals was studied by energy-dispersive X-ray spectroscopy, which showed inhomogeneous distribution of the ceria concentration along the length of the crystal. The displacement of the dopant along the height of the ingot during crystallization led to an almost twofold difference in the ceria concentrations at the beginning and end of the ingot. Therefore, to study the structure and measure the transport characteristics, the samples were cut from the middle of ingots, where the concentration of cerium and scandium oxides corresponded to their content in the initial batch.

An analysis of the density and microhardness of the crystals (Table 1) shows that co-doping with ceria leads to a decrease in their density and an increase in microhardness compared with those in the crystals stabilized only by scandium oxide. At a fixed ceria concentration in crystals, their density decreases, and the microhardness increases with the concentration of scandium oxide.

The X-ray diffraction (XRD) analysis showed that the 8Sc1CeSZ and 9Sc1CeSZ crystals are tetragonal, while the 10Sc1CeSZ crystal has a cubic structure. Table 2 shows the lattice parameters of the xSc1CeSZ crystals under study and, for comparison, the crystals of the xScSZ series. It can be seen that co-doping with ceria leads to an increase in the a lattice parameter, while the c parameter decreases as compared to that in the crystals stabilized only by scandium oxide. Accordingly, the degree of tetragonality $\left(c/\sqrt{2}a\right)$ of the crystals decreases, and the crystal structure parameters of 8Sc1CeSZ and 9Sc1CeSZ become closer to those of a cubic structure than the parameters of 8ScSZ and 9ScSZ. Because of the larger ionic radius of Ce^{4+} compared to that of Zr^{4+}, the lattice parameter of the cubic phase in the 10Sc1CeSZ crystal is larger than in 10ScSZ. Table 2 also shows the lattice parameters of the crystals after annealing at 1200°C because the annealing of xSc1CeSZ crystals in air leads to the $Ce^{3+} \rightarrow Ce^{4+}$ transition and can affect the parameters of their structure. According to the data of Table 2, the decrease in the concentration of trivalent cerium cations after annealing affected the structure parameters only in the 8Sc1CeSZ crystal. The degree of tetragonality of the 8Sc1CeSZ crystal after annealing increased, which is associated with a decrease in the size of cerium ions during the $Ce^{3+} \rightarrow Ce^{4+}$ transition and a decrease in the number of vacancies because the replacement of the Zr^{4+} ion by Ce^{4+} in the lattice does not require charge compensation. In the 9Sc1CeSZ and 10Sc1CeSZ crystals with high contents of scan-

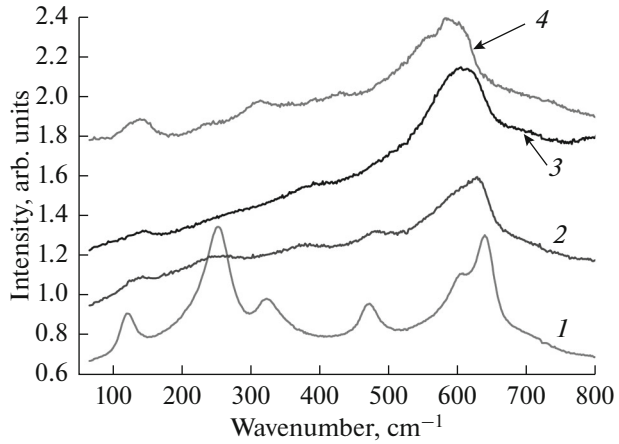

Fig. 2. Raman spectra of $(ZrO_2)_{1-x-y}(Sc_2O_3)_x(CeO_2)_y$ crystals: (*1*) 8Sc1CeSZ, (*2*) 9Sc1CeSZ, (*3*) and (*4*) various sections of the 10Sc1CeSZ crystal.

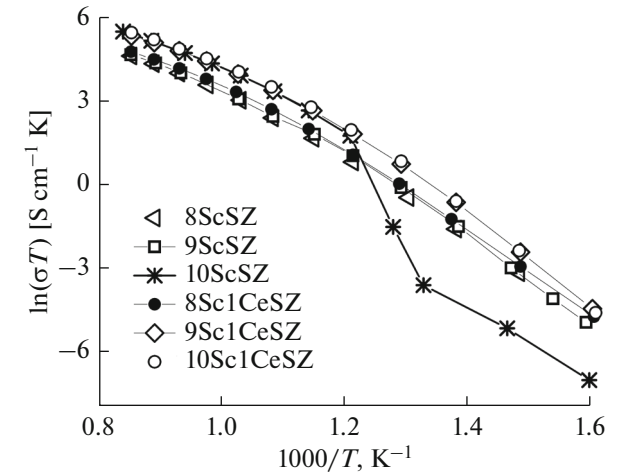

Fig. 3. Temperature dependences of the specific bulk conductivity of $(ZrO_2)_{1-x}(Sc_2O_3)_x$ and $(ZrO_2)_{1-x-y}(Sc_2O_3)_x(CeO_2)_y$ crystals.

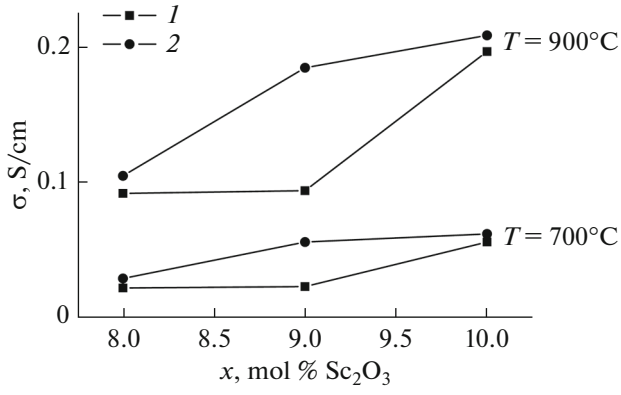

Fig. 4. Comparison of the ion conductivity of crystals σ at 700°C and 900°C: (*1*) $(ZrO_2)_{1-x}(Sc_2O_3)_x$ and (*2*) $(ZrO_2)_{1-x-y}(Sc_2O_3)_x(CeO_2)_y$.

dium oxide, the structure parameters did not change after annealing.

The phase composition of *x*Sc1CeSZ crystals was also studied by Raman spectroscopy (Fig. 2). The spectrum of the 8Sc1CeSZ and 9Sc1CeSZ crystals corresponds to the spectrum of the tetragonal crystals, which agrees with the XRD data. For the 10Sc1CeSZ crystal, however, regions with a rhombohedral structure were detected by Raman spectroscopy in addition to the cubic phase. Figure 2 shows two Raman spectra for the 10Sc1CeSZ sample obtained from different regions of the crystal; the spectra of the cubic and rhombohedral phases differ substantially [18]. The presence of the rhombohedral phase in the 10Sc1CeSZ crystal was found predominantly in its upper part, which may be due to the increased concentration of cerium oxide at the end of the ingot due to the displacement of the impurity during crystallization.

Figure 3 shows the temperature dependences of the specific conductivity of the 8Sc1CeSZ, 9Sc1CeSZ, and 10Sc1CeSZ crystals under study in the Arrhenius coordinates and, for comparison, the similar dependences of 8ScSZ, 9ScSZ, and 10ScSZ. A comparison of the conductivities of the 8Sc1CeSZ and 9Sc1CeSZ crystals with those of 8ScSZ and 9ScSZ shows that co-doping with cerium oxide increases the conductivity; for crystals with 9 mol % Sc_2O_3, the increase is more significant than for crystals with 8 mol % Sc_2O_3 (Fig. 4). The increase in conductivity may be associated with the structure of the 8Sc1CeSZ and 9Sc1CeSZ crystals, namely, with a lower degree of tetragonality than in 8ScSZ and 9ScSZ crystals. The heating of the crystals in air at 950°C while burning-in the platinum paste to deposit the electrodes will lead to a change in the degree of tetragonality of 8Sc1CeSZ, in contrast to the structure of the 9Sc1CeSZ crystals, so the difference in the conductivity of the 8ScSZ and 8Sc1CeSZ crystals is much smaller than for the 9ScSZ and 9Sc1CeSZ crystals. The introduction of 1 mol % CeO_2 in the crystals stabilized with 10 mol % Sc_2O_3 removes the jump on the temperature dependence of the specific bulk conductivity related to the transition from rhombohedral to cubic phase at ~550°C. The conductivity of the 10Sc1CeSZ crystals is higher than that of 10ScSZ over the whole temperature range.

Thus, the co-doping of crystals with ceria increases the conductivity in the range of compositions under study, but an increase in their specific electric conductivity depends on the Sc_2O_3 content in the initial composition and is determined by the phase composition of the crystals.

CONCLUSIONS

The crystals of $(ZrO_2)_{1-x}(Sc_2O_3)_x(CeO_2)_{0.01}$ (x = 0.08–0.10) solid solutions were obtained by directional crystallization. It was shown that the crystals of the grown compositions were translucent, opalescent,

without cracks, and with different microstructures in the bulk. It was impossible to obtain optically homogeneous, fully transparent crystals in the range of compositions under study. At a crystallization rate of 10 mm/h, there is nonuniform distribution of ceria along the length of the ingot.

According to the XRD analysis, the co-doping of crystals with cerium oxide increases the stability of the tetragonal phases and decreases the tendency toward the formation of the low-symmetric rhombohedral phase compared with the crystals stabilized only by scandium oxide.

It was shown that the introduction of cerium oxide in an amount of 1 mol % increases the conductivity of the crystals, but the increase in their electric conductivity depends on the Sc_2O_3 content in the initial composition and is determined by the phase composition of the crystals. The 10Sc1CeSZ crystals containing a cubic phase have the highest conductivity.

ACKNOWLEDGMENTS

This study was financially supported by the Russian Scientific Foundation (project no. 16-13-00056).

REFERENCES

1. Goodenough, J.B., Oxide-ion electrolytes, *Annu. Rev. Mater. Res.*, 2003, vol. 33, p. 91.
2. Kharton, V.V., Marques, F.M.B., and Atkinson, A., Transport properties of solid oxide electrolyte ceramics: a brief review, *Solid State Ionics*, 2004, vol. 174, p. 135.
3. Omar, S., and Bonanos, N., Ionic Conductivity Ageing Behaviour of 10 mol % Sc_2O_3–1 mol % CeO_2–ZrO_2 Ceramics, *J. Mater. Sci.*, 2010, vol. 45, p. 6406.
4. Kumar, A., Jaiswal, A., Sanbui, M., and Omar, S., *Scr. Mater.*, 2016, vol. 121, p. 10.
5. Lee, D.-S., Kim, W.S., Choi, S.H., Kim, J., Lee, H.-W., and Lee, J.-H. Characterization of ZrO_2 co-doped with Sc_2O_3 and CeO_2 electrolyte for application of intermediate temperature SOFCs, *Solid State Ionics*, 2005, vol. 176, p. 33.
6. Wang, Z., Cheng, M., and Bi, Z., Structure and impedance of ZrO_2 doped with Sc_2O_3 and CeO_2, *Mater. Lett.*, 2005, vol. 59, p. 2579.
7. Omar, S., Najib, W.B., Chen, W., and Bonanos, N., Electrical conductivity of 10 mol % Sc_2O_3–1 mol % M_2O_3–ZrO_2 ceramics, *J. Am. Ceram. Soc.*, 2012, vol. 95, p. 1965.
8. Liu, M., He, C., Wang, J., Wang, W.G., and Wang, Z., Materials for intermediate temperature solid oxide fuel cell, *J. Alloys Compd.*, 2010, vol. 502, p. 319.
9. Abbas, H.A., Argirusis, C., Kilo, M., Wiemhöfer, H.D., Hammad, F.F., and Hanafi, Z.M., Preparation and conductivity of ternary scandia-stabilised zirconia, *Solid State Ionics*, 2011, vol. 184, p. 6.
10. Tan, J., Su, Y., Tang, H., Hu, T., Yu, Q., Tursun, R., and Zhang, X., Effect of calcined parameters on microstructure and electrical conductivity of 10Sc1CeSZ, *J. Alloys Compd.*, 2016, vol. 686, p. 394.
11. Liu, M., He, C.R., Wang, W.G., and Wang, J.X., Synthesis and characterization of 10Sc1CeSZ powders prepared by a solid-liquid method for electrolyte-supported solid oxide fuel cells, *Ceram. Int.*, 2014, vol. 40, p. 5441.
12. Lee, D., Lee, I., Jeon, Y., Song, R., Characterization of scandia stabilized zirconia prepared by glycine nitrate process and its performance as the electrolyte for ITSOFC, *Solid State Ionics*, 2005, vol. 176, p. 1021.
13. Borik, M.A., Bredikhin, S.I., Bublik, V.T., Kulebyakin, A.V., Kuritsyna, I.E., Lomonova, E.E., and Tabachkova, N.Y. The impact of structural changes in ZrO_2–Y_2O_3 solid solution crystals grown by directional crystallization of the melt on their transport characteristics, *Mater. Lett.*, 2017, vol. 205, p. 186.
14. Osiko, V.V., Borik, M.A., and Lomonova, E.E., Synthesis of Refractory Materials by Skull Melting Technique, in *Springer Handbook of Crystal Growth*, 2010, Part B, p. 433.
15. Borik, M.A., Bredikhin, S.I., Kulebyakin, A.V., Kuritsyna, I.E., Lomonova, E.E., Milovich, F.O., Myzina, V.A., Osiko, V.V., Panov, V.A., Ryabochkina, P.A., Seryakov, S.V., and Tabachkova, N.Yu., Melt growth, structure and properties of $(ZrO_2)_{1-x}(Sc_2O_3)_x$ solid solution crystals (x = 0.035–0.11), *J. Cryst. Growth*, 2016, vol. 443, p. 54.
16. Kuz'minov, Yu.S., Lomonova, E.E., and Osiko, V.V., *Tugoplavkie materialy iz holodnogo tiglja* (Refractory Materials from Cold Crucible), Moscow: Nauka, 2004.
17. Borik, M.A., Bredikhin, S.I., Bublik, V.T., Kulebyakin, A.V., Kuritsyna, I.E., Lomonova, E.E., Milovich, F.O., Myzina, V.A., Osiko, V.V., Ryabochkina, P.A., Seryakov, S.V., and Tabachkova, N.Yu., Phase composition, structure and properties of $(ZrO_2)_{1-x-y}(Sc_2O_3)_x(Y_2O_3)_y$ solid solution crystals (x = 0.08–0.11; y = 0.01–0.02) grown by directional crystallization of the melt, *J. Cryst. Growth*, 2017, vol. 457, p. 122.
18. Fujimori, H., Yashima, M., Kakihana, M., and Yoshimura, M., β-Cubic phase transition of scandia-doped zirconia solid solution: Calorimetry, X-ray diffraction, and Raman scattering, *J. Appl. Phys.*, 2002, vol. 91, p. 6493.

Translated by L. Smolina